Version of Record: https://www.sciencedirect.com/science/article/pii/S1364032120303944
Manuscript_59085329ccf88d6df31b76fc9139ebaa

Humans in the city: representing outdoor thermal comfort in urban canopy models

Pigliautile I.[1], Pisello A. L.[1-2 *], Bou Zeid E.[3]

[1]CIRIAF - Interuniversity research centre on pollution and environment Mauro Felli – Department of engineering, University of Perugia, 06125, Italy

[2] Department of Engineering, University of Perugia, Perugia, 06125, Italy

[3] Department of Civil and Environmental Engineering, Princeton University, NJ, United States

ABSTRACT

The negative effects of urban heat islands (UHIs) on citizens' well-being and life quality are widely acknowledged, but they still represent critical challenges, particularly since urban population is predicted to rise to 60% of the world population by 2030. Computational models have become useful tools for addressing these challenges and investigating urban microclimate repercussions on citizens' comfort and urban liveability. Despite that humans typically remain absent from such models. This work bridges this gap, moving beyond purely thermodynamic Urban Canopy Models (UCMs) to highlight the importance of integrating even simplified pedestrians' biophysics for comfort assessment. Human physiology parameterization is therefore introduced into the Princeton Urban Canopy Model (PUCM), which had been designed to investigate the effect of greenery and novel materials on the UHI. Human thermal comfort is assessed in terms of the skin temperature and then evaluated against the apparent temperature, a widely-used thermal comfort indicator. Different configurations of the same urban canyon are therefore tested to assess the effectiveness of cool materials and trees for human thermal comfort enhancement. Results show that cool skins in the canyon's built environment lead to an air temperature reduction up to 1.92 K, but slightly worsen human comfort in terms of a warmer computed skin temperature by 0.27 K. The indirect effect of trees, that exclude shading, are negligible for human thermal comfort. The new integrated human-centric model can help policymakers and urban planners to easily

* Corresponding author details, anna.pisello@unipg.it

assess the potential benefits or threats to citizens' well-being associated with specific urban configurations.

HIGHLIGHTS

1. Parametrized human physiology in Princeton Urban Canopy Model for outdoor comfort
2. Computed skin temperature as indicator of heat-related health hazards of citizens
3. Novel indicator combined to internationally recognized apparent temperature
4. Non-careful cool paving and facades design may compromise pedestrians' well-being
5. Mitigation strategies should be designed also according to pedestrians when needed

KEYWORDS

Urban microclimate, Urban Heat Island, Urban Heat Mitigation, Thermal Comfort, Human Energy Balance.

WORD COUNT: 5670

LIST OF ABBREVIATIONS

	Nomenclature	**Units**
UHI	Urban Heat Island	-
HW	Heat Wave	-
WRF	Weather Research Forecasting model	-
MCM	Microclimate Models	-
UCM	Urban Canopy Model	-
PUCM	Princeton Urban Canopy Model	-
R	Net radiation	[W/m^2]
C	Convection exchange	[W/m^2]
K	Conduction through the skin layer	[W/m^2]
E	Evaporative latent heat loss	[W/m^2]
LW	Longwave radiation	[W/m^2]
SW	Shortwave radiation	[W/m^2]
a_{sw}	absorption coefficient of the human body	-

θ_z	solar zenith angle	rad
θ_z	solar azimuth angle	rad
H	Building height	[m]
HB	Pedestrian height	[m]
X	Human body location within the canyon	[m]
T_a	Air temperature	[°C]
T_{sk}	Skin temperature	[°C]
T_{cr}	Human core temperature	[°C]
h_c	Convective coefficient	[W/(m^2 K)]
h_e	Evaporative heat transfer coefficient	[W/(m^2 Pa)]
F_{clC}	Clothing thermal efficiency factor	-
F_{pcl}	Clothing permeation efficiency factor	-
e	Air vapour pressure	[Pa]
e_{sk}	Saturation vapor pressure at T_{sk}	[Pa]
w	Skin wetness	-
m_{sw}	Sweat mass production rate	[kg/(h m^2)]
L_w	Latent heat coefficient of water vaporization	[Wh/kg]
R_d	Vapor diffusion resistance	[Pa h/kg]
ws	Wind speed	[m/s]
AT	Apparent temperature	[°C]

1. Introduction

Urban areas are undergoing continuous growth in terms of inhabitants and land use expansion: 68% of world population is expected to live in urban areas by 2050 according to the 2018 Revision of World Urbanization Prospect [1]. The urbanization process implies a modification of land use and cover, and a consequent alteration of the site-specific energy balance as pointed out by Oke in [2]. Such changes lead to the well-known phenomenon of Urban Heat Island (UHI) meaning that urban regions experience higher temperature with respect to their rural surroundings. This impact of the urban fabric on the environment has several negative effects on citizens' life quality which are becoming an increasing concern as stated in the review study of Filho et al. [3]. In fact, it is now well established that UHI directly impacts building energy consumption and pollutants concentration. The existence of an impact-chain of air pollution-urban heat island-heating energy use was recently confirmed

for the Beijing urban area through a coupling of the Building Effect Parameterization-Building Energy Model in WRF to a single building energy model by Xu et al. [4]. Through an extensive monitoring campaign conducted in Athens, Greece, Koronakis et al. [5] demonstrated that buildings located in urban areas affected by a UHI require up to double the cooling of their rural counterparts, thus tripling peak electricity load for cooling purposes. Moreover, high temperatures observed in urban contexts threaten dwellers health in various regions and climates as already highlighted in the 2010 review paper by Hajat and Kosatky [6]. More recent progress on the urban overheating impact on mortality and morbidity and urban vulnerability projections in a climate change framework are discussed in the 2020 review of Santamouris [7]. As a matter of fact, an increasing trend of heat-related deaths consistent with a rising frequency of heat-waves per year is shown by Bandala et al. in Las Vegas for 2007 to 2016 [8]. A detailed statistical analysis on urban extreme temperatures impact on human health for the period 2007-2014 was also performed for Cyprus in Pyrgou and Santamouris work [9]. Taylor et al. [10] estimated that 21% of mortality was due to the UHI effect during summertime in the West Midlands region of the UK, correlating mortality to the estimated maximum temperature computed for the actual urbanized conditions compared with conditions with no urban surfaces. A different approach, coupling remote sensing and field survey, is implemented in the research study by Mirzaei at al. for monitoring the UHI impact on citizens' health status in Isfahan, Iran [11].

As already briefly stated, the rising concern on urban overheating and human health and social responsibility [12] are tightly linked to the on-going change in the climate, which is going to further exacerbate the negative consequences of the UHI phenomenon. More frequent and more intense extreme weather events such as thunderstorms and heat weaves (HW) are expected in the near future [13]. In particular, UHI and HW synergistically interact as shown through a combination of observational and modelling analyses in Li and Bou-Zeid [14], and more recently confirmed by Zhao et al. for a much larger number of cities [15]. The combination of the two phenomena further exacerbates urban population morbidity as documented by the extensive amount of research summarized in the critical review of Campbell et al. [16]. Nevertheless, the built environment is characterized by high-heterogeneity and each city has its own morphology (i.e. physical structure and dimensions of the urban fabric), metabolism (i.e. material characteristics, and energy and water consumption), and climate (e.g. precipitation, incoming radiation, regional temperatures). The combination of a city's morphology, metabolism, and climate generates a specific spatial

distribution and temporal variation of the temperature and wind fields, affecting comfort level and air quality in the city. A formal definition of these intra-urban microclimate peculiarities was proposed by Stwart and Oke, who identified prototypical Local Climate Zone (LCZ) that encompass all land cover/land use typologies they found in cities [17]. Nevertheless, more complex patterns of the intra-urban microclimate variations are experimentally observed through in-field monitoring along transects at pedestrian level in different urban contexts by Pigliautile and Pisello [18]. Temporal and spatial variations are also observed by coupling different satellite observations, vehicular transects monitoring and computer simulation for the specific case of a desert city in the work of Zhou et al. [19]. Therefore, the LCZ concept, very useful for modelling purposes, does not fully explain variability in atmospheric conditions in cities. More recently, Llaguno-Munitxa and Bou-Zeid [20] proposed the concept of an environmental neighborhood as the surrounding area that significantly influences environmental quality at a given point in the city, and proposed a method to delineate these neighborhoods. The spatial variability of temperature along such environmental neighbourhoods leads to differential risk levels, which may be coupled to different socioeconomic status of inhabitants, yielding an even higher vulnerability in specific location as highlighted by Zafeiratou et al. [21].

Therefore, scale-dependent built-environment effects cannot be neglected in a sustainable and comfortable urban development [22]. A huge effort of the scientific community has been devoted to find tailored and suitable countermeasures to the UHI phenomenon in the last decades [23]. Nowadays, the most common UHI mitigation strategies concern the implementation of cool materials and the introduction of greenery in the urban environment [24]. In the first case, treated urban surfaces reflect a large amount of the incoming shortwave radiation keeping urban surfaces “cooler”. The potential of cool roofs to reduce heat-related mortality due to UHI during heatwaves by up to 25% is demonstrated in [25]. Rosso et al. also proposed innovative “cool” materials suitable for historic sites where aesthetical constrains could limit the applicability of this mitigation technique [26]. On the other hand, implementation of greenery or permeable surfaces contributes to reduce UHI by means of evapotranspiration and the increase of latent heat exchanges in the urban energy balance [27].

Within this framework, climate and weather models are useful tools for a deeper understanding of the urban environment that emerges from the complex interaction between land and atmosphere. Such models are of particular interest for the assessment of adaptive measures efficacy from the initial design phase. Urban climate models are thus recognized as

fundamental pillars among existing software for a comprehensive analysis of cities behaviour and the selection of proper adaptation techniques [28]. As a matter of fact, Johari et al. suggested the integration of building energy models with other models, such as climate and outdoor models, as the main route to improve the accuracy in urban building energy simulations [29]. Mauree et al. [30] identified four modelling domains that have to be considered: urban climate, building energy demand, outdoor thermal comfort, and energy systems. Nevertheless, the same authors highlighted that these models do not easily communicate among each other, leading to complex and time-consuming processes. Recently, new studies have proposed comprehensive digital workflow by integrating different tools [31], but they are still limited in number. In this view, Coccolo et al. presented a modelling procedure to assess the impact of trees on outdoor thermal comfort in the Swiss International Scientific School of Dubai, and demonstrated the potential to significantly reduce the extent of thermally uncomfortable hours through the use of greenery [32].

The current work fully integrates for the first time two of the above-mentioned domains, i.e. urban climate and outdoor thermal comfort, by introducing a simplified scheme of the human body into the Princeton Urban Canopy Model (PUCM). The aim of the work is thus to contribute to enhancing urban sustainability through including human comfort dimension in the urban climate simulation framework. The PUCM solves the energy budget of a parameterized urban canopy layer and simulates the heterogeneity of built surfaces with sub-facets for different materials and detailed representations of hydrological processes [33]. Recent additions to the code also allow to assess the impact of adaptive materials characterized by dynamic thermal behaviour such as thermochromic materials [34]. More details concerning the specific implementation of the UCM and other urban climate models are given in section the following subsection which focuses on existing typologies of microclimate models and their more common applications, and which highlights the gap related to direct representation of pedestrians' comfort in these models. In section 2, the developed model that computes the human energy budget is presented. Results concerning thermal comfort assessment in six different configurations of the same canyon are provided in section 3. The various tested configurations allow to check the effectiveness of cool finishing on canyon walls and/or ground, and the potential of introducing trees in the canyon section for ameliorating the thermal comfort of citizens.

The original contribution therefore consists of the formulated model itself, its integration into the UCM, and the novel analyses. This research framework, for the first time, includes human

body thermal balances in a UCM, opening up the possibility to downscale urban energy fluxes and to consider their effect on pedestrians, thus providing a simple and effective tool to guide policymaking and urban planning.

1.1 Microclimate models and their applications

The increasing awareness of specific urban microclimatic conditions [35] and their negative impact on both building energy consumption and citizens' well-being [36] prompted the increasing investigation of thermal behaviour of cities from the design stage of buildings construction to broader urban planning [37]. Urban microclimate models are the proper tools for assessing the impact of new constructions or the implementation of tailored adaptive strategies on the city environment. In particular, two kinds of models are generally coupled to achieve high-accuracy in the assessment of local climate in complex and heterogeneous urban contexts: (i) meteorological mesoscale models, such as the Weather Research Forecasting model (WRF) [38], and (ii) microclimate models (MCMs) computing heat, momentum, and mass exchanges in the urban environment. This approach allows to assess and predict UHI spatio-temporal patterns across heterogeneous urban areas, and how they are coupled to weather extremes and global climate change [39].

There are two common typologies of MCMs: (i) models solving the airflow pattern inside the canopy layer by means of computational fluid dynamics (CFD) [40], and (ii) Urban Canopy Models (UCMs) that only solve for the energy and water budget of the urban canopy layer, with coupling to a coarse atmospheric model above that layer [41]. Among the CFD models, ENVI-met, developed by Michael Bruse at the Rurh University of Bochum [42], is one of the most widely employed tools for microclimate investigation [43]. Conry et al. [44] used one-way dynamical downscaling to assess Chicago's Heat Island under a changing climate by sequential downscaling from (i) the Global Climate Community Atmosphere Model [45], to (ii) the regional climate WRF model, and finally to (iii) the microscale ENVI-met model. Outdoor thermal comfort analysis is also provided through an ENVI-met tool specifically dedicated to thermal-comfort assessment. Kleerekoper et al. highlighted potentials of 3D ENVI-met models in investigating the impact of urban design measures on citizens' thermal comfort in their review [46]. Nevertheless, microclimate CFD models require extensive computational power so they are not easily coupled with long-term downscaling analyses. On the other hand, UCMs are based on the parameterization of the urban environment [47] and as such they require a relatively lower computational effort for long-term analysis coupled with

WRF, while guaranteeing a sufficiently accurate analysis of the urban microclimate since they resolve all the built-surfaces interaction with the atmosphere [48]. Huidong et al. coupled WRF and UCM to quantify UHI intensity in terms of simulated 2-m air temperature across Berlin [49] and a similar approach was used by Teixeira et al. for Lisbon [50]. Grimmond at al. [51] provide a detailed comparative analysis among 33 international urban energy balance models concluding that model complexity does not always lead to a better performance and that generally these schemes are able to reproduce all-wave radiation well, but are less capable in latent heat flux modelling. The Princeton UCM (PUCM) adopted in this study was developed specifically to address this shortcoming: it resolves all the important water storage and flux terms in the urban canopy to improve the latent heat flux and its associated evaporative cooling [52]. As a matter of fact, due to the detailed representation of urban heterogeneity and hydrological processes, the PUCM allows to assess the impervious surface contribution to urban evaporation after rainfall events [53], to analyse the heavy convective rainfall by reproducing a more detailed surface energy balance than traditional slab models [54], and to realistically represent trees and associated physical processes such as shortwave/longwave radiation exchange, sensible and latent heat exchange, and root water uptake [55],

Therefore, the combination of UCM and WRF models allows the assessment of the spatio-temporal variation of UHI intensity with acceptable resolution [56] and the analysis of cooling effects due to an extensive application of adaptation strategies [57]. A further step in the research commonly include the analysis of related variation in building energy consumptions by coupling mesoscale, MCMs, and Building Energy Models as presented in the review by Lauzet et al. [58]. Nevertheless, few studies adopt these numerical models to investigate human comfort in outdoors, even if it is highly compromised by the UHI. Morris et al. [59] adopt WRF 3.5.1 coupled with UCM to analyse urbanization influence on urban outdoor thermal discomfort, but this is done by means of direct comfort indexes that do not consider human thermoregulatory response or human energy balance [60].

The current work aims to fill this gap by introducing, for the first time, a simplified physiological scheme of the human body into the PUCM. We then apply the model to assess whether the computed interfacial skin temperature, a good indicator of thermal comfort perception of the pedestrian, can be accurately surrogated for by the apparent temperature, a widely-adopted index of thermal comfort that does not involve a human model [61].

Subsequently, we investigate the effectiveness of various heat mitigation measures in improving thermal comfort in a prototypical urban canyon.

2. Research Method

Urban microclimate coupled to climate change is a threat for citizens' well-being. The human body in urban outdoors is exposed to high thermal stress correlated to urban morphology and built surfaces materials. The PUCM adopts an advanced surface exchange scheme, coupling mass and energy transport within the urban canopy layer. Previous work has demonstrated the model's accuracy and has already used it as a tool to assess the effectiveness of UHI mitigation strategies [33]. This work introduces a simplified scheme of the human body in the PUCM in order to add information on human thermal comfort and perception since it is highly compromised by UHI. The following sections present in detail the developed model and the chosen boundaries for the simulation tests including six different configurations of the same canyon that progressively vary the optical properties of its facets and add trees.

2.1 Model description

The human body scheme implemented in the PUCM is a single mass model with a constant core temperature and an outer skin shell with negligible thermal inertia, which is an accurate assumption if the skin is conceptualized as a thin layer. All through the paper, heat fluxes are defined positive into the skin and negative out of the skin. The simplified human energy balance is then expressed by the sum of the energy fluxes exchanged between the pedestrian and the environment (all in W/m^2). For the skin, an interfacial energy balance can then be described using the following equation:

$$R + C + K + E = 0 \tag{1}$$

where R is the radiative exchange between the body and the environment, C is the energy flux by convection, K is the conductive flux of heat from the core to the surface, and E is the latent heat loss due to evapotranspiration at the skin surface. The above equation is solved as a 4th order (due to the outgoing longwave radiation depending on the temperature to the power 4) polynomial for T_{sk}, i.e. skin layer temperature, to enforce the energy balance. To capture the fast response of the human body to external stimuli, equation 1 is solved with a time step dt = 1 s. More details about each term of the energy budget are given in the following subsections.

2.1.1 Net radiation, R

The net radiation term comprises both longwave and shortwave radiation budgets, and the shortwave contribution is partitioned between direct and diffuse components as expressed in equation 2.

$$R = LW_{in} + LW_{out} + a_{sw}(SW_{dir} + SW_{diff}) \text{ [W/m}^2\text{]} \quad (2)$$

where LW_{in} and LW_{out} are the incoming and outgoing longwave radiations respectively; a_{sw} is the absorption coefficient (1 − albedo) of the human body for shortwave radiation; SW_{dir} and SW_{diff} are the direct and diffuse components of the incoming shortwaves. To computeSW_{dir}, the incident direct solar radiation is weighted by the fraction of the exposed human body surface projected perpendicular to the sunrays direction. This is computed geometrically assuming the human body as a cylinder of 1.8 m height and with a total surface of 2 m^2 [62]. The procedure takes into account the solar zenith angle (θ_z), solar azimuth angle relative to canyon orientation (θ_a), building height (H), pedestrian height (HB), and location of the human body within the canyon (X). Adapting the method already proposed by Ryu [55] for trees, six reference angles are considered to distinguish among fully shaded, fully sunlit or partially sunlit condition of the body.

The diffuse shortwave component of the radiative budget SW_{dff} is computed by considering multiple Lambertian reflections of sunrays off the walls and ground, up to two times. No selective reflectance components are considered in this study [63]. More specifically, the amount of diffuse shortwave radiation reaching the pedestrian depends on a-priori imposed radiative properties of the canyon facets and their view factors with both the sky and the human body. Thus, view factors between the human body and surroundings are required. In order to generate a simple, but reliable model, the pedestrian is discretized into 5 equidistant points. The view factors obtained at each single point are then averaged assuming different weighing coefficient based on the represented portion of the body: head, chest (2 points), and legs (2 points) from the top to the bottom respectively. Based on these assumptions, a weight of 0.1 is given to human legs, less sensitive to thermal stress, 0.3 to chest points, representative of a larger surface, and 0.2 to the head.

Longwave radiation budget comprises the radiation emitted by surrounding surfaces as function of their computed interfacial temperatures and the measured longwave radiation incoming from the sky. The emitted term, i.e. LW_{out}, has a small contribution from the

reflected longwave (−(1 − emissivity) LW_{in}), but it is mainly a function of the fourth power of T_{sk}, the unknown variable of the polynomial equation.

2.1.2 Convection exchange, C

The convective exchange between the pedestrian and the environment depends on temperature differentials between the human body's outer layer and the ambient air temperature, i.e. T_{sk} and T_a, respectively, as well as on wind velocity that will dictate the proper convective coefficient h_c (Equation 3).

$$C = F_{clC}\, h_c(T_a - T_{sk}) \ [W/m^2] \quad (3)$$

where F_{clcC} is the clothing thermal efficiency factor, which takes into account the effect of clothing insulation on the considered energy exchange [64].

2.1.3 Conduction through the skin layer, K

The conduction term expresses the energy flux into the skin envelope due to thermal differences between the core and the skin itself as presented by Equation 4.

$$K = K_{min}\, (T_{cr} - T_{sk})/dx \ [W/m^2] \quad (4)$$

where K_{min} is the minimum heat conductance of the skin tissue and dx is a pre-defined thickness of the outer shell of the human body in which the temperature is not equal to the core temperature. The authors tested different values of shell thickness during the first phase of model robustness check and decided to set a pre-defined value of 2 cm since it was found to yield the most realistic results for the skin temperature fluctuations. This assumption yielded a reliable fluctuation of the indicator adopted for the assessment of thermal comfort within the canyon, i.e. the interfacial skin temperature. We need to underline that this outer shell is not the human skin organ, which is much thinner: This outer shell represents the thickness of the layer over which the temperature varies (linearly) from the outer skin temperature to the constant core temperature, a sort of a "thermal skin".

2.1.1 Evaporative latent heat loss, E

In addition to sensible heat exchanges, the human body releases energy to the outdoors by evaporation at the skin surface. In particular, the total latent heat flux considered in Equation 1 (E) encompasses (i) the latent heat lost by diffusion through the skin, i.e. E_{diff}, and (ii) latent

heat due to regulatory sweating, i.e. E_{sw}. Both processes are related to the maximum evaporative heat loss that could be sustained by the human body with a given skin temperature in a given environment, where the ambient air temperature and specific humidity are known quantities. This upper threshold of evaporative exchange (a potential evaporation) is therefore proportional to the concentration gradient of water vapor from the skin surface, assumed as saturated in water vapor for this maximum, to the ambient air as described by the Equation 5.

$$E_{max} = h_e \cdot F_{pcl} (e - e_{sk}) \ [W/m^2] \quad (5)$$

where h_e is the evaporative heat transfer coefficient for water vapor in [W/(m^2 Pa)], F_{pcl} the clothing permeation efficiency factor, e the ambient water vapor pressure in [Pa], and e_{sk} the saturation vapor pressure at skin temperature in [Pa]. The skin might not be at saturation or could be rather dry; the ratio between the actual evaporation heat loss and its maximum value represents the skin wetness (w), which ranges between 1 (max evaporation) to 0.06 (min evaporation). The lower wetness limit occurs in absence of regulatory sweating, when the evaporative heat loss at skin surface is entirely due to vapor diffusion [65]. The evaporative term of the human energy balance is therefore expressed by the following equation (Equation 6):

$$E = E_{sw} + E_{diff} = (-L_w \cdot m_{sw}) + L_w \cdot [(1-w) \cdot (e_{sk} - e)]/R_d \ [W/m^2] \quad (6)$$

where L_w is the latent heat coefficient of water vaporization at body temperature, R_d is the resistance to vapor diffusion defined as a constant and expressed in [Pa·h/kg] and m_{sw} is the mass of sweat produced by the human body in [kg/(h·m^2)] computed according to skin temperature variation with respect to comfort conditions, i.e. skin temperature equal to 34.1 °C. If the skin is wet from sweating, the first term dominates and the second terms is zero. As w drops below one, the sweating is concomitantly reduced. In accordance with complex physiological models, the body sweat production is related to variation of both skin and core temperature of the human body. To make the model more robust, the latent heat component is modelled explicitly, i.e., the saturation water vapor e_{sk} at the current time step is computed using the skin temperature at the previous time step. Given that the time step is 1 s, this approach should be very accurate since the variation of T_{sk} from one step to the next is very small.

2.2 Simulation setup

The developed code is tested under weather conditions during the hottest week of summer 2012 in Princeton (NJ, USA). The selected period, i.e. July 3rd to 9th, encompasses seven consecutive days with registered air temperatures above 30 °C, and an absolute maximum of 39 °C. Environmental data are collected at a dedicated, roof-mounted weather station every 30 minutes. Figure 1 summarizes simulation boundary conditions in terms of weather forcing above the urban canopy; they represent the atmospheric conditions PUCM interacts with. PUCM then computes the in-canyon air temperature, humidity and wind speed, and our physiological model and computation of apparent temperature use these in-canyon parameters.

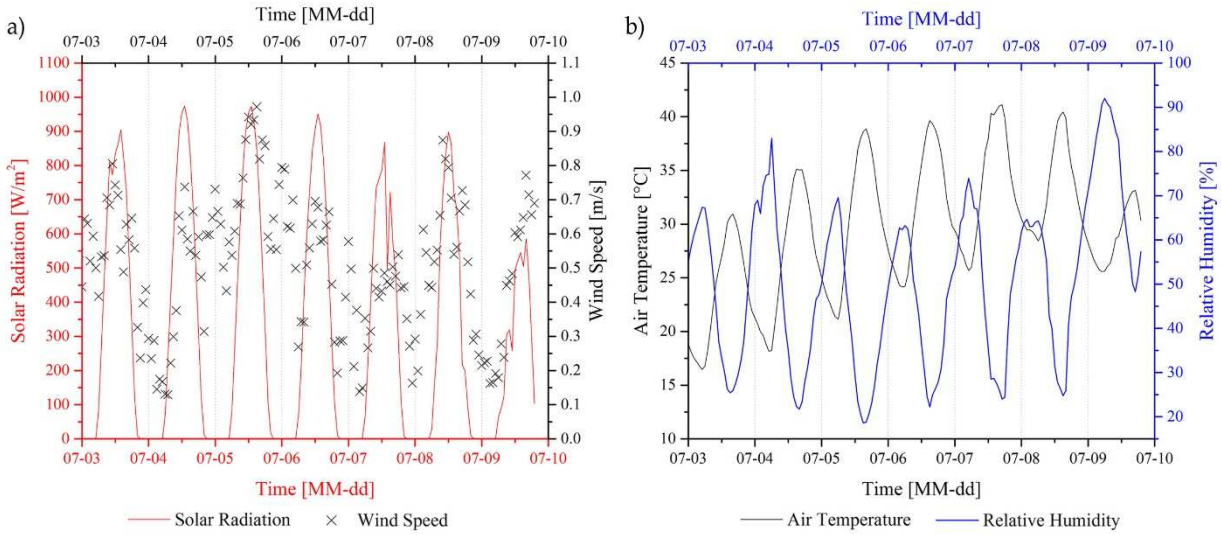

Figure 1. Simulation weather forcing in terms of: (a) incoming global radiation and wind speed; and (b) observed air temperature and relative humidity.

The considered urban canyon is North-East/South-West oriented and presents an aspect ratio, i.e. building height to canyon width, of 1.3 representative of a uniform street canyon according to literature [66]. Given the above-mentioned characteristics, six different configurations are tested based on a reference scenario with no greenery and where all the model facets have a low value of albedo, i.e. 0.25 and 0.15 for walls and ground respectively. The optical characteristics of the urban facets are progressively modified, and trees are included in the section of the urban canyon. The proposed combinations are summarized in Figure 2 where dark and light colours for walls and ground represent dark and cool finishing materials applied on each specific surface. Albedo for cool materials is set to 0.65 and 0.45 for walls and ground respectively according to literature [67]. The simulated trees are the ones already implemented in the PUCM and presented by Ryu at al. in [55]. The tree fraction in the

along-canyon axis is set to 0.2, i.e. a tree every 5 m. Trees impact the simulated environment since the PUCM computes all the physical processes related to radiative exchanges, including mutual shading and multiple reflections, and sensible and latent exchanges, the latest occurring through transpiration. Nevertheless, this work aims to show the specific indirect impact of trees on human comfort without considering the benefit of the provided shade on the human body energy balance if the pedestrian is under the tree. Therefore, the human is assumed to be away from the trees.

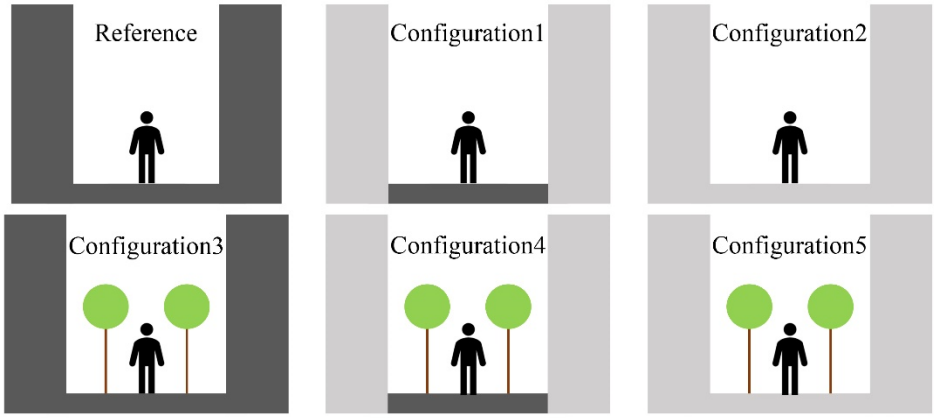

Figure 2. Scheme of the six analysed configurations characterized by different albedo of the urban facets and presence or absence of trees. Note that our pedestrian is not shaded at all, assumed not to be located directly under a tree despite the two-dimensional depiction in the figure.

Finally, the developed code also quantifies outdoor thermal comfort by computing the apparent temperature, which is one of the most complete indicators according to the literature [60]. Indeed, this internationally recognized parameter of apparent temperature corrects the air temperature by accounting for all the environmental parameters affecting thermal perception including relative humidity, expressed through the water vapour pressure, wind speed, and the radiative exchange environment by means of the net radiation received per unit area of body surface. The adopted formula is the following (Equation 7) [68]:

$$AT = T_a + (0.348 \cdot e)/100 - 0.7ws + 0.7R/(ws + 10) - 4.25\ [°C] \quad (7)$$

where T_a it the dry bulb temperature in [°C], ws the wind speed in [m/s], and e the water vapor pressure in [hPa]. This indicator can then be compared to the skin temperature, which is a more faithful and direct measure of thermal comfort.

3. Results and discussion

The current section reports the results of the investigation in terms of the human energy balance components and the computed interfacial skin temperature. Figure 3 shows the results concerning two out of the five simulated days, i.e. July 5th and 6th, chosen as representative of the general trend for the reference simulated scenario.

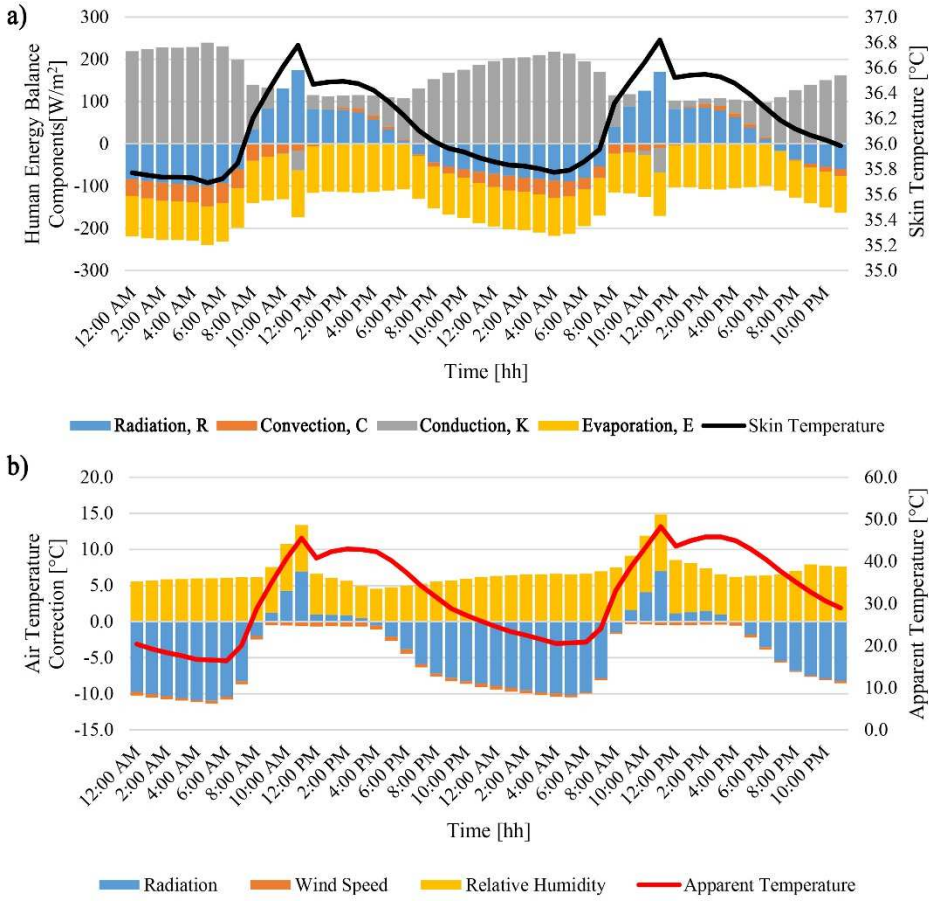

Figure 3. Hourly trends of: (a) computed interfacial skin temperature; and (b) apparent temperature deviation from air temperature. They are combined with bar plots of: (a) each human skin thermal balance component; and (b) the contribution of each environmental parameter to the air temperature correction, yielding apparent temperature for the reference scenario.

Computed skin temperature (Figure 3a) fluctuates between 35.6 °C and 36.8 °C. These values are always above the comfort threshold provided in literature, i.e. around 34.4 °C. This could be a consequence of the implemented method that simplifies human physiology, without taking into account specific thermoregulatory systems such as the variability of the core temperature, or simply a reflection of the fact that during this extreme heat event the person cannot attain thermal comfort. Nevertheless, the computed skin temperature trend is

reasonable, and it enhances the energy loss due to conduction through the skin layer from the core to the outdoor during night-time when the contributions of radiative and convective exchanges are negative and the skin is cooler. Evaporation implies always an energy loss and is therefore always negative and almost constant, meaning that the major contribution obtained with the implemented model is given by diffusion rather than sweat production in the current simple version of the model. This might indicate that sweating models that are better adapted to the current formulation are needed, if the ones used here did not predict sweating despite the thermal discomfort.

Results for apparent temperature are then presented, taking into account that a higher value of this parameter reflects more thermal loading/input into the energy balance model. **Errore. L'origine riferimento non è stata trovata.**b shows hourly values of all the terms that are considered to correct the observed air temperature into an equivalent perceived value; the latter is also presented in the graph. In particular, the correction-terms labels refer to the observed environmental parameter specifically considered for the apparent temperature calculation. The radiative environment plays a major role in the computed apparent temperature at night when surrounding surfaces temperature drops and no incoming shortwave is available. Such negative components lead to a perceived temperature lower than the actual air temperature. Radiative contribution is somewhat less significant during day-time when it induces a maximum temperature increment of 7.4 K when solar radiation impinges directly on the human body. Relative humidity contribution is always positive and it ranges between 4 K and 11.6 K, while wind speed negatively affects temperature perception causing a maximum reduction of only –0.7 K.

Computed interfacial skin temperature and apparent temperature are well correlated as depicted in Figure 4a, which distinguishes between the night-time and day-time to point out the different contribution of incoming shortwave radiation. Plotted values are the hourly averages for the whole simulated week and for all tested configurations. This agreement is a good indicator of the validity of the developed physiological model. Stronger linear correlation is observed at night with a correlation coefficient R^2 of 0.96, while more scattered values are observed in presence of incoming shortwave radiation yielding a lower value of R^2 equal to 0.86. A direct comparison between the two parameters with respect to simulated air temperature is also given in Figure 4b. This graph allows to evaluate the neutral and hazardous thermal conditions for the human body expressed by the interfacial skin temperature. In particular, comfortable conditions are represented by a skin temperature up to

36 °C while progressively warmer perception corresponds to higher values of the parameter. Four levels of comfort, i.e. LC1 to LC4, are also shown in Figure 4b for identifying thresholds in between two consequent levels of needed precaution, i.e. LC1=caution, LC2=extreme caution, LC3=danger, LC4=extreme danger, as reported in previous research [69] in terms of AT.

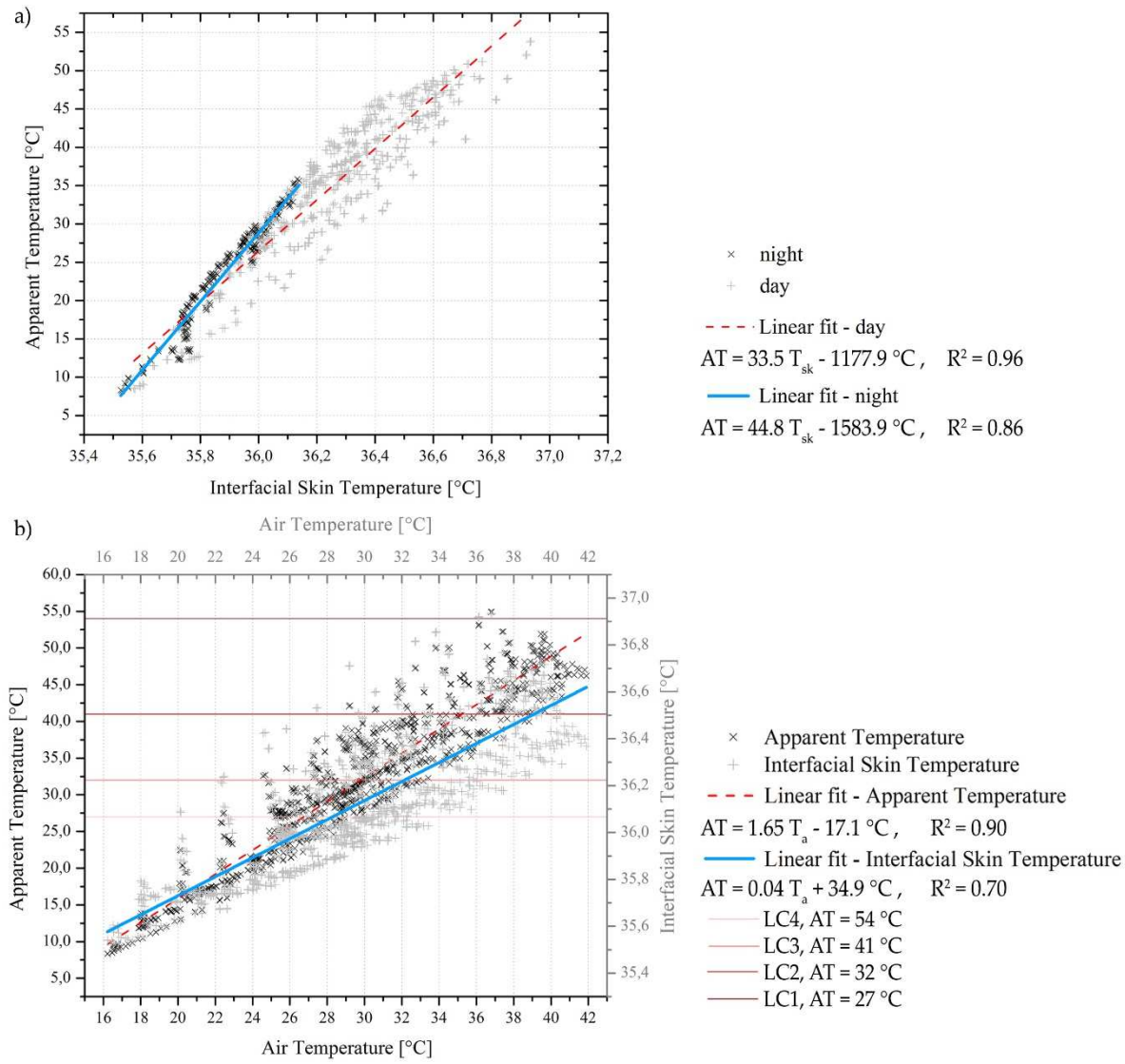

Figure 4. (a) Apparent temperature and skin temperature correlation distinguishing between night- and day-time; (b) Apparent and skin temperature with respect to in canyon air temperature distinguishing among all the tested configurations, and depicting the LC levels typically adopted to categorize thermal comfort.

Hourly air and skin temperature differentials from five mitigated scenarios with respect to the reference one are shown in Figure 5 for the hottest simulated day. Air temperature (for the in-canyon air) variations depict the UHI mitigation effect of the implemented strategies during

both day-time and night-time. The lower absorbed shortwave radiation produces up to 1.6 °C of air temperature reduction for configuration 1 with implemented cool walls, while the shadowing effect coupled with transpiration due to trees causes a smaller decrease of −0.6 °C in configuration 3 with dark canyon surfaces. Configuration 5, which combines high albedo and trees, result in the largest air cooling of up to 2°C. Nevertheless, human comfort seems to be worsened by the implementation of cool materials within the urban canyon. Higher reflectivity increases the amount of diffuse shortwave reaching the human body during day-time, while the minor reduction in longwave emitted by surrounding surfaces, kept to lower temperatures due to the cool finishing, does not produce comparable benefits in the computed energy budget. Moreover, the indirect (since the human is not shaded) effect of trees, clearly shown from observed air temperature drops, is not as effective in reducing thermal stress. This leads to negligible, but worsening, variations in skin temperature in all the simulated scenarios.

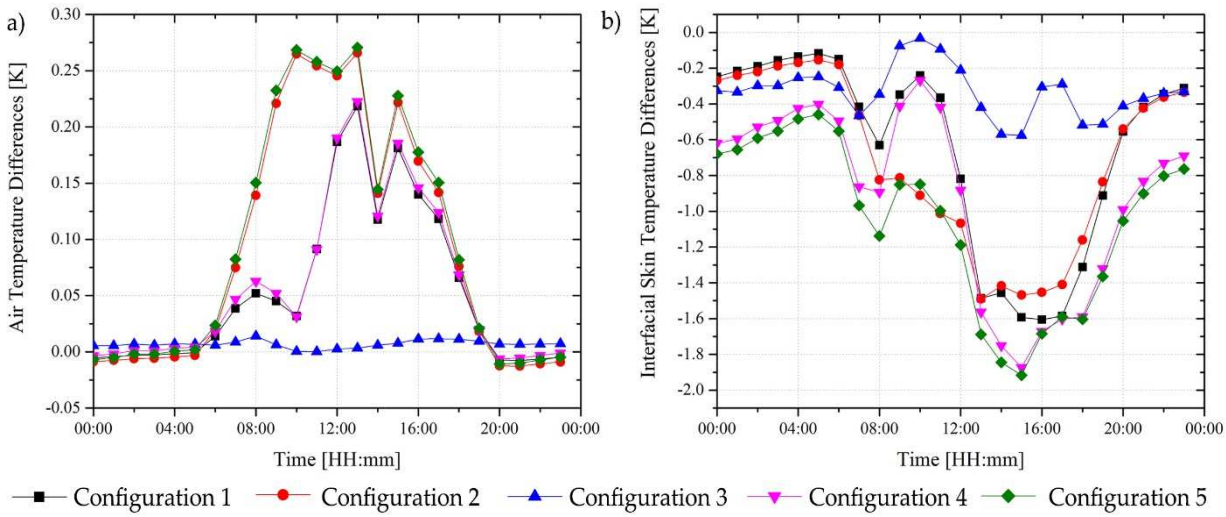

Figure 5. Hourly differentials from the mitigated configurations with respect to reference scenario for the hottest simulated day of: (a) air temperature and (b) interfacial skin temperature.

Focusing on human thermal comfort, Figure 6 shows hourly values of each individual component of the human energy balance for all the six simulated configurations. Once more, the outlined results confirm the negative impact associated with the implementation of cool surfaces within the urban canyon, mainly imputable to higher contribution of the radiative component of the energy balance. Indeed, the convective heat losses between the human body and the environment intensify in “cool scenarios”, but the magnitude of this beneficial effect, i.e. maximum observed reduction of −6 W/m^2 in that same configuration 5, is negligible compared to the radiative increase, i.e. maximum gain of +79 W/m^2 in configuration 5.

Significant changes are not observed in terms of evaporative exchange, while the conduction term varies in accordance with the simulated human body model showing particularly uncomfortable conditions during day-time. Specifically, the conductive flux from 10 a.m. to 4 p.m. is always negative for scenarios with both cool walls and ground. This means that the body core is gaining heat and the pedestrian health therefore deteriorates.

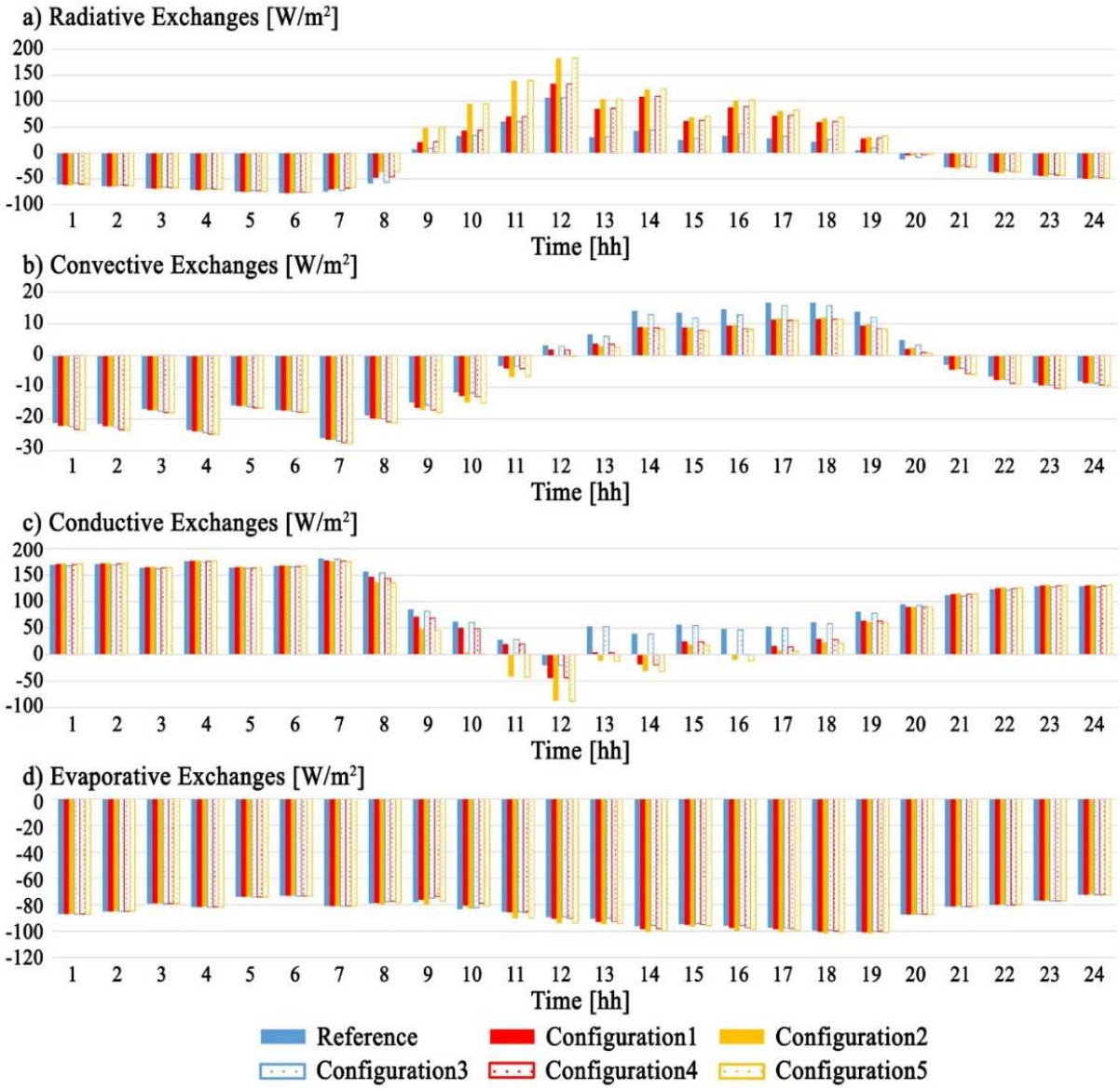

Figure 6. Hourly contribution for all the six simulated configurations of each component of the human energy balance: (a) radiation, (b) convection, (c) conduction, and (d) evaporation.

4. Conclusions

The assessment of citizens' thermal comfort, particularly under climate warming or urban expansion projections is needed starting at the design stage of a careful urban planning. To

avoid complex work-flows, this study introduces the pedestrian perspective within the Princeton Urban Canopy Model. In particular, the manuscript presents a simplified single mass human body model assuming a constant core temperature and a skin shell with negligible thermal inertia. The interfacial skin temperature, obtained by solving the human energy budget, represents thermal comfort perception of the pedestrian within the modelled canyon. The reliability of the computed indicator is demonstrated by comparison to the internationally recognized apparent temperature.

The novel code is then used for computing thermal comfort variation due to the application of different UHI mitigation strategies, i.e., varying façade albedo and trees in the canyon section. Canyon air temperature reductions up to −1.92 K, are observed for the tested configuration that includes (i) cool finishing on both ground and walls and (ii) the introduction of trees in the street section. Nevertheless, pedestrian comfort is compromised during day-time by the higher amount of radiative exchanges due to the higher reflection of cool materials implemented on walls and ground.

This is the first coupling, to the best knowledge of the authors, of a physiological thermal comfort model into a UCM. It enables a direct calculation of the skin temperature of a pedestrian in the canyon, and while such a value is in fact personalized and depends on activity and physiology and maybe on modelling assumptions, the influence of mitigation measures on its value are robust. As such, the model serves the purpose it was designed for, i.e., informing planners and decision makers about the impact of urban overheating mitigation strategies on thermal comfort. These impacts, as our paper clearly shows, can be counterintuitive with some measures that reduce air temperatures in fact deteriorating thermal comfort. More broadly, the model can now be implemented into WRF or other Earth System Models to introduce the important human dimension into these geophysical models.

As further development, direct contribution of trees to human comfort enhancement will be tested in the future by including shadowing effect on the pedestrian. Moreover, alternative finishing materials of canyon surfaces will be tested with the final aim to find a good compromise between UHI mitigation and outdoor spaces liveability. The human thermal balance model can also be improved, particularly regarding latent heat cooling via sweating.

5. Acknowledgement

The authors wish also to thank H2CU for the great international cooperation opportunities of College Italia. Also, they wish to thank the UNESCO Chair on Water management and culture for fostering such urban studies. The study is partially supported by SOS CITTA' (Fondazione Cassa di Risparmio di Perugia, 2018.0499.026). Prof. Elie Bou-Zeid is supported by the NOAA-Princeton Cooperative Institute for Climate Science and by the US National Science Foundation under Grant No. 1664091 and the UWIN Sustainability Research Network Cooperative Agreement 1444758.

6. List of References

[1] UN DESA. 2018 Revision of World Urbanization Prospects. 2018.

[2] Oke TR. The energetic basis of the urban heat island. R Meteorol Soc 1982;108:1–24. doi:10.1109/ICTD.2009.5426693.

[3] Leal Filho W, Echevarria Icaza L, Neht A, Klavins M, Morgan EA. Coping with the impacts of urban heat islands. A literature based study on understanding urban heat vulnerability and the need for resilience in cities in a global climate change context. J Clean Prod 2018;171:1140–9. doi:10.1016/j.jclepro.2017.10.086.

[4] Xu X, González JE, Shen S, Miao S, Dou J. Impacts of urbanization and air pollution on building energy demands — Beijing case study. Appl Energy 2018;225:98–109. doi:10.1016/J.APENERGY.2018.04.120.

[5] Koronakis I, Assimakopoulos D., Santamouris M, Argiriou A, Georgakis C, Papanikolaou N, et al. On the impact of urban climate on the energy consumption of buildings. Sol Energy 2002;70:201–16. doi:10.1016/s0038-092x(00)00095-5.

[6] Hajat S, Kosatky T. Heat-related mortality: a review and exploration of heterogeneity. J Epidemiol Community Heal 2010;64:753–60. doi:10.1136/jech.2009.087999.

[7] Santamouris M. Recent progress on urban overheating and heat island research. Integrated assessment of the energy, environmental, vulnerability and health impact. Synergies with the global climate change. Energy Build 2020;207:109482. doi:10.1016/j.enbuild.2019.109482.

[8] Bandala ER, Kebede K, Jonsson N, Murray R, Green D, Mejia JF, et al. Extreme heat and mortality rates in Las Vegas, Nevada: inter-annual variations and thresholds. Int J Environ Sci Technol 2019;16:7175–86. doi:10.1007/s13762-019-02357-9.

[9] Pyrgou A, Santamouris M. Increasing Probability of Heat-Related Mortality in a Mediterranean City Due to Urban Warming. Int J Environ Res Public Health 2018;15:1571. doi:10.3390/ijerph15081571.

[10] Taylor J, Wilkinson P, Picetti R, Symonds P, Heaviside C, Macintyre HL, et al. Comparison of built environment adaptations to heat exposure and mortality during hot weather, West Midlands region, UK. Environ Int 2018:287–94. doi:10.1016/j.envint.2017.11.005.

[11] Mirzaei M, Verrelst J, Arbabi M, Shaklabadi Z, Lotfizadeh M. Urban Heat Island Monitoring and Impacts on Citizen's General Health Status in Isfahan Metropolis: A Remote Sensing and Field Survey Approach. Remote Sens 2020;12:1350. doi:10.3390/rs12081350.

[12] Xu X, Taylor JE, Pisello AL. Network synergy effect: Establishing a synergy between building network and peer network energy conservation effects. Energy Build 2014;68:312–20. doi:10.1016/j.enbuild.2013.09.017.

[13] Sheridan SC, Allen MJ. Changes in the Frequency and Intensity of Extreme Temperature Events and Human Health Concerns. Curr Clim Chang Reports 2015;1:155–62. doi:10.1007/s40641-015-0017-3.

[14] Zhao L, Oppenheimer M, Zhu Q, Baldwin JW, Ebi KL, Bou-Zeid E, et al. Interactions between urban heat islands and heat waves. Environ Res Lett 2018;13.

[15] Zhao L, Oppenheimer M, Zhu Q, Baldwin JW, Ebi KL, Bou-Zeid E, et al. Interactions between urban heat islands and heat waves. Environ Res Lett 2018;13. doi:10.1088/1748-9326/aa9f73.

[16] Campbell S, Remenyi TA, White CJ, Johnston FH. Heatwave and health impact research: A global review. Heal Place 2018;53:210–8. doi:10.1016/j.healthplace.2018.08.017.

[17] Stewart ID, Oke TR. Local climate zones for urban temperature studies. Bull Am Meteorol Soc 2012;93:1879–900. doi:10.1175/BAMS-D-11-00019.1.

[18] Pigliautile I, Pisello AL. Environmental data clustering analysis through wearable sensing techniques: New bottom-up process aimed to identify intra-urban granular morphologies from pedestrian transects. Build Environ 2020;171:106641. doi:10.1016/j.buildenv.2019.106641.

[19] Zhou B, Kaplan S, Peeters A, Kloog I, Erell E. “Surface,” “satellite” or “simulation”: Mapping intra-urban microclimate variability in a desert city. Int J Climatol 2020;40:3099–117. doi:10.1002/joc.6385.

[20] Llaguno-Munitxa M, Bou-Zeid E. The environmental neighborhoods of cities and their spatial extent. Environ Res Lett 2020. doi:10.1088/1748-9326/ab8d7e.

[21] Zafeiratou, Analitis, Founda, Giannakopoulos, Varotsos, Sismanidis, et al. Spatial Variability in the Effect of High Ambient Temperature on Mortality: An Analysis at Municipality Level within the Greater Athens Area. Int J Environ Res Public Health 2019;16:3689. doi:10.3390/ijerph16193689.

[22] Georgescu M, Chow WTL, Wang ZH, Brazel A, Trapido-Lurie B, Roth M, et al. Prioritizing urban sustainability solutions: coordinated approaches must incorporate scale-dependent built environment induced effects. Environ Res Lett 2015;10:061001. doi:10.1088/1748-9326/10/6/061001.

[23] Akbari H, Kolokotsa D. Three decades of urban heat islands and mitigation technologies research. Energy Build 2016;133:834–52. doi:10.1016/j.enbuild.2016.09.067.

[24] Taleghani M. Outdoor thermal comfort by different heat mitigation strategies- A review. Renew Sustain Energy Rev 2018;81:2011–8. doi:10.1016/j.rser.2017.06.010.

[25] Macintyre HL, Heaviside C. Potential benefits of cool roofs in reducing heat-related mortality during heatwaves in a European city. Environ Int 2019;127:430–41. doi:10.1016/J.ENVINT.2019.02.065.

[26] Rosso F, Golasi I, Castaldo VL, Piselli C, Pisello AL, Salata F, et al. On the impact of

innovative materials on outdoor thermal comfort of pedestrians in historical urban canyons. Renew Energy 2018;118. doi:10.1016/j.renene.2017.11.074.

[27] Dai Z, Guldmann J-M, Hu Y. Thermal impacts of greenery, water, and impervious structures in Beijing's Olympic area: A spatial regression approach. Ecol Indic 2019;97:77–88. doi:10.1016/J.ECOLIND.2018.09.041.

[28] Keirstead J, Jennings M, Sivakumar A. A review of urban energy system models: Approaches, challenges and opportunities. Renew Sustain Energy Rev 2012;16:3847–66. doi:10.1016/j.rser.2012.02.047.

[29] Johari F, Peronato G, Sadeghian P, Zhao X, Widén J. Urban building energy modeling: State of the art and future prospects. Renew Sustain Energy Rev 2020;128:109902. doi:10.1016/j.rser.2020.109902.

[30] Mauree D, Naboni E, Coccolo S, Perera ATD, Nik VM, Scartezzini JL. A review of assessment methods for the urban environment and its energy sustainability to guarantee climate adaptation of future cities. Renew Sustain Energy Rev 2019;112:733–46. doi:10.1016/j.rser.2019.06.005.

[31] Naboni E, Natanian J, Brizzi G, Florio P, Chokhachian A, Galanos T, et al. A digital workflow to quantify regenerative urban design in the context of a changing climate. Renew Sustain Energy Rev 2019;113:109255. doi:10.1016/j.rser.2019.109255.

[32] Coccolo S, Pearlmutter D, Kaempf J, Scartezzini JL. Thermal Comfort Maps to estimate the impact of urban greening on the outdoor human comfort. Urban For Urban Green 2018;35:91–105. doi:10.1016/j.ufug.2018.08.007.

[33] Wang ZH, Bou-Zeid E, Smith JA. A coupled energy transport and hydrological model for urban canopies evaluated using a wireless sensor network. Q J R Meteorol Soc 2013;139:1643–57. doi:10.1002/qj.2032.

[34] Fabiani C, Pisello AL, Bou-Zeid E, Yang J, Cotana F. Adaptive measures for mitigating urban heat islands: The potential of thermochromic materials to control roofing energy balance. Appl Energy 2019;247:155–70. doi:10.1016/j.apenergy.2019.04.020.

[35] RIZWAN AM, DENNIS LYC, LIU C. A review on the generation, determination and mitigation of Urban Heat Island. J Environ Sci 2008;20:120–8. doi:10.1016/S1001-0742(08)60019-4.

[36] Li X, Zhou Y, Yu S, Jia G, Li H, Li W. Urban heat island impacts on building energy consumption: A review of approaches and findings. Energy 2019;174:407–19. doi:10.1016/J.ENERGY.2019.02.183.

[37] Gago EJ, Roldan J, Pacheco-Torres R, Ordóñez J. The city and urban heat islands: A review of strategies to mitigate adverse effects. Renew Sustain Energy Rev 2013;25:749–58. doi:10.1016/j.rser.2013.05.057.

[38] Skamarock C, Klemp B, Dudhia J, Gill O, Liu Z, Berner J, et al. A Description of the Advanced Research WRF Model Version 4 2019. doi:10.5065/1DFH-6P97.

[39] Ching JKS. A perspective on urban canopy layer modeling for weather, climate and air quality applications. Urban Clim 2013;3:13–39. doi:10.1016/j.uclim.2013.02.001.

[40] Toparlar Y, Blocken B, Maiheu B, van Heijst GJF. A review on the CFD analysis of urban microclimate. Renew Sustain Energy Rev 2017;80:1613–40. doi:10.1016/j.rser.2017.05.248.

[41] Mirzaei PA. Recent challenges in modeling of urban heat island. Sustain Cities Soc 2015;19:200–6. doi:10.1016/j.scs.2015.04.001.

[42] Bruse M, Fleer H. Simulating surface–plant–air interactions inside urban environments with a three dimensional numerical model. Environ Model Softw 1998;13:373–84. doi:10.1016/S1364-8152(98)00042-5.

[43] Tsoka S, Tsikaloudaki A, Theodosiou T. Analyzing the ENVI-met microclimate model's performance and assessing cool materials and urban vegetation applications–A review. Sustain Cities Soc 2018;43:55–76. doi:10.1016/j.scs.2018.08.009.

[44] Conry P, Sharma A, Potosnak MJ, Leo LS, Bensman E, Hellmann JJ, et al. Chicago's Heat Island and Climate Change: Bridging the Scales via Dynamical Downscaling. J Appl Meteorol Climatol 2015;54:1430–48. doi:10.1175/JAMC-D-14-0241.1.

[45] Collins WD, Rasch PJ, Boville BA, Hack JJ, McCaa JR, Williamson DL, et al. The

Formulation and Atmospheric Simulation of the Community Atmosphere Model Version 3 (CAM3). J Clim 2006;19:2144–61. doi:10.1175/JCLI3760.1.

[46] Kleerekoper L, Taleghani M, van den Dobbelsteen A, Hordijk T. Urban measures for hot weather conditions in a temperate climate condition: A review study. Renew Sustain Energy Rev 2017;75:515–33. doi:10.1016/j.rser.2016.11.019.

[47] Garuma GF. Review of urban surface parameterizations for numerical climate models. Urban Clim 2018;24:830–51. doi:10.1016/j.uclim.2017.10.006.

[48] Mauree D, Blond N, Clappier A. Multi-scale modeling of the urban meteorology: Integration of a new canopy model in the WRF model. Urban Clim 2018;26:60–75. doi:10.1016/J.UCLIM.2018.08.002.

[49] Li H, Zhou Y, Wang X, Zhou X, Zhang H, Sodoudi S. Quantifying urban heat island intensity and its physical mechanism using WRF/UCM. Sci Total Environ 2019;650:3110–9. doi:10.1016/j.scitotenv.2018.10.025.

[50] Teixeira JC, Fallmann J, Carvalho AC, Rocha A. Surface to boundary layer coupling in the urban area of Lisbon comparing different urban canopy models in WRF. Urban Clim 2019;28:100454. doi:10.1016/J.UCLIM.2019.100454.

[51] Grimmond CSB, Blackett M, Best MJ, Barlow J, Baik J-J, Belcher SE, et al. The International Urban Energy Balance Models Comparison Project: First Results from Phase 1. J Appl Meteorol Climatol 2010;49:1268–92. doi:10.1175/2010JAMC2354.1.

[52] Ramamurthy P, Bou-Zeid E, Smith JA, Wang Z, Baeck ML, Saliendra NZ, et al. Influence of Subfacet Heterogeneity and Material Properties on the Urban Surface Energy Budget. J Appl Meteorol Climatol 2014;53:2114–29. doi:10.1175/JAMC-D-13-0286.1.

[53] Ramamurthy P, Bou-Zeid E. Contribution of impervious surfaces to urban evaporation. Water Resour Res 2014;50:2889–902. doi:10.1002/2013WR013909.

[54] Ryu Y-H, Smith JA, Bou-Zeid E, Baeck ML. The Influence of Land Surface Heterogeneities on Heavy Convective Rainfall in the Baltimore–Washington Metropolitan Area. Mon Weather Rev 2016;144:553–73. doi:10.1175/MWR-D-15-

0192.1.

[55] Ryu YH, Bou-Zeid E, Wang ZH, Smith JA. Realistic Representation of Trees in an Urban Canopy Model. Boundary-Layer Meteorol 2016;159:193–220. doi:10.1007/s10546-015-0120-y.

[56] Li H, Zhou Y, Wang X, Zhou X, Zhang H, Sodoudi S. Quantifying urban heat island intensity and its physical mechanism using WRF/UCM. Sci Total Environ 2019;650:3110–9. doi:10.1016/J.SCITOTENV.2018.10.025.

[57] Rossi F, Anderini E, Castellani B, Nicolini A, Morini E. Integrated improvement of occupants' comfort in urban areas during outdoor events. Build Environ 2015;93:285–92. doi:10.1016/j.buildenv.2015.07.018.

[58] Lauzet N, Rodler A, Musy M, Azam MH, Guernouti S, Mauree D, et al. How building energy models take the local climate into account in an urban context – A review. Renew Sustain Energy Rev 2019;116:109390. doi:10.1016/j.rser.2019.109390.

[59] Morris KI, Chan A, Morris KJK, Ooi MCG, Oozeer MY, Abakr YA, et al. Impact of urbanization level on the interactions of urban area, the urban climate, and human thermal comfort. Appl Geogr 2017;79:50–72. doi:10.1016/J.APGEOG.2016.12.007.

[60] Coccolo S, Kämpf J, Scartezzini J-L, Pearlmutter D. Outdoor human comfort and thermal stress: A comprehensive review on models and standards. Urban Clim 2016;18:33–57. doi:10.1016/j.uclim.2016.08.004.

[61] G. Steadman R. A Universal Scale of Apparent Temperature. J Appl Meteorol - J APPL METEOROL 1984;23:1674–87. doi:10.1175/1520-0450(1984)023<1674:AUSOAT>2.0.CO;2.

[62] Tikuisis P, Meunier P, Jubenville CE. Human body surface area: Measurement and prediction using three dimensional body scans. Eur J Appl Physiol 2001;85:264–71. doi:10.1007/s004210100484.

[63] Han Y, Taylor JE, Pisello AL. Exploring mutual shading and mutual reflection inter-building effects on building energy performance. Appl Energy 2017;185:1556–64. doi:10.1016/j.apenergy.2015.10.170.

[64] BURTON AC, EDHOLM OG. Man in a cold environment. Physiological and pathological effects of exposure to low temperatures. Man a Cold Environ Physiol Pathol Eff Expo to Low Temp 1955.

[65] Brebner DF, Kerslake M, Waddell JL, Waddell JL. THE DIFFUSION OF WATER VAPOUR THROUGH HUMAN SKIN. J Physiol 1956;132:225–31.

[66] Shishegar N. Street Design and Urban Microclimate: Analyzing the Effects of Street Geometry and Orientation on Airflowand Solar Access in Urban Canyons. J Clean Energy Technol 2013;1:52–6. doi:10.7763/jocet.2013.v1.13.

[67] Castaldo VL, Rosso F, Golasi I, Piselli C, Salata F, Pisello AL, et al. Thermal comfort in the historical urban canyon: The effect of innovative materials. Energy Procedia, vol. 134, 2017, p. 151–60. doi:10.1016/j.egypro.2017.09.553.

[68] Steadman RG. A Universal Scale of Apparent Temperature. J Clim Appl Meteorol 1984;23:1674–87.

[69] Overcenco A, Pantea V. Study on extreme heat biometeorological conditions impacting human health. J Hyg Public Heal 2012;62:29–37.